ISSN 2394-3777 (Print)
ISSN 2394-3785 (Online)
Available online at www.ijartet.com
International Journal of Advanced Research Trends in Engineering and Technology (IJARTET)
Vol. 3, Special Issue 22, April 2016

TRIBOLOGICAL STUDY ON PLA/CS REINFORCED BASALT FIBER COMPOSITES USING FUZZY CLUSTERING ALGORITHM

Arul Jeya Kumar A and Srinivasan V

Department of Manufacturing Engineering, Annamalai University, Annamalai Nagar-608002.

Corresponding Author: Arul Jeya Kumar A. Mobile: +919443265623; Email:aruljeyakumar@yahoo.co.in

Abstract

The tribological behaviour of chitosan (CS) filled polylactic acid (PLA)/ basalt fiber (BF) reinforced (PBC) composites of three different volume fraction were studied using Pin-on-Disc wear tester under dry sliding conditions. The worn out surfaces of the composites were examined by scanning electron microscope (SEM) and wear mechanisms dominating each sliding conditions were classified. The wear maps were used to study the influence of sliding velocity and normal force over the Co-efficient of friction (μ), contact temperature (CT) and wear rate (WR). A wear mechanism map was developed by using Fuzzy C- Means Clustering Algorithm Method (FCM) to study the wear mechanism of composites. Results showed increased weight percentage of basalt and chitosan in PLA played a vital role in increasing the wear resistance.

Keywords: PLA/Basalt/Chitosan Composites; Pin-On-Disc; Wear Rate; Wear mechanism maps; Coefficient of friction; Contact temperature; Scanning Electron Microscope (SEM).

1. Introduction

The advance technology focus on sustaining natural environment and green chemistry leads the development of the next generation of materials, products and processes. In the today's world, the need for application of environmentally friendly biodegradable polymers, especially produced from renewable resources, is increasingly coming to focus [1-4]. Hence natural fibers are suggested due to its low cost, bio friendly and renewable characteristics [5-6].

Polylactic acid (PLA) is a firm thermoplastic that has a special interest as a matrix in hybrid Composite materials. PLA is a highly recommended biopolymer and is highlighted because it is derived from a renewable resource such as corn, wheat, rice, potato, tapioca. It also has good mechanical properties, tensile strength of 60 MPa, tensile modulus of 3 GPa. PLA parts reinforced with

ISSN 2394-3777 (Print)
ISSN 2394-3785 (Online)
Available online at www.ijartet.com
International Journal of Advanced Research Trends in Engineering and Technology (IJARTET)
Vol. 3, Special Issue 22, April 2016

natural plant fibers found to have slight increase in mechanical parameters due to the temperature and shear sensitive property of the natural plant fibers [7]. A possible alternative for the natural plant fibers is the mineral basalt fibers [8]. Tensile strength of basalt fiber tends to increase with increasing drawing temperatures due to increasing proportions of crystal nuclei of basalt at lower temperatures [9]. The increasing application of basalt fiber raised the question whether basalt fiber is harmful to health. Kogan et al made rats inhale air containing asbestos and basalt fibers for 6 months. According to the results, basalt fibers seem to be a good selection to reinforce PLA composites [10].

Chitosan is a linear polysaccharide composed of randomly distributed D-glucosamine (deacetylated unit) and N-acetyl-D-glucosamine. Chitosan and its derivatives are very attractive candidates as scaffold composites because they apparently degrade as new tissues are formed, without inflammatory reactions or toxic degradation [11]. Kim et al. [12] noted that chitosan has been extensively used in bone tissue engineering because of its capacity to promote growth and mineral rich matrix deposition by osteoblasts in culture. Also, chitosan is biocompatible and biodegradable. Besides its biodegradability and biocompatibility, Chitosan is reported to be an active polymer with antimicrobial activity [13].

The use of composites as another class of engineering materials is very vital to the success of any industrialized nation. Numerous research institutes adopted the challenge of developing and improving the existing composites. Record available shows that the present global consumption is continually increasing [14 & 15]. Hence natural fibers are suggested due to its low cost, bio friendly and renewable characteristics [16].

2. Materials and Methods

2.1 Materials:

Poly lactic acid (PLA) biopolymer 3052 D designed for injection moulding application in pellet form was obtained from Nature-Tec India Pvt Ltd., Chennai, Tamilnadu, India. It was dried at 120°C for 6 hours prior to extrusion. Significantly higher adhesion could be developed between the phases, because the residual moisture could induce degradation and it could also weaken the adhesion between the fibers and the matrix material. The basalt fiber used in this work was supplied from Muktagiri Industrial Corporation, Borivali West, Mumbai, India, and it was supplied as silane treated, developed specially for strong adhesion with Poly lactic acid (PLA). The average diameter of the fibers was 13 μm and length about 4-6 mm. The Basalt fiber was also dried along with the PLA resin to remove residual moisture. High molecular weight chitosan (CS) with high

ISSN 2394-3777 (Print)
ISSN 2394-3785 (Online)
Available online at www.ijartet.com
International Journal of Advanced Research Trends in Engineering and Technology (IJARTET)
Vol. 3, Special Issue 22, April 2016

degree of deacetylation was supplied by Axogen pvt Limited (Pudhucherry, India). A cutter grinder was employed to reduce the particle size of CS powder from 715 µm to 180 µm.

2.2 Blending of PLA/CS:

There are some challenges to overcome when using small-sized CS polysaccharides in extrusion process. The main challenges are the difficult feeding of the material into the extruder and the tendency of tiny materials to agglomerate when dry, due to the formation of hydrogen bonds. One possibility for overcoming these problems is to use adequate solvent oil to mix Poly lactic acid (PLA) and Chitosan (CS) Powder homogenously during compounding. Required amount of Poly lactic acid (PLA) and Chitosan (CS) Powder was mixed by adding acetone, which acts as an adhesive agent for PLA and CS that suits for feeding in extruder.

2.3 Fabrication of hybrid composite:

Fabrication of basalt fiber reinforced PLA/CS hybrid bio composite consists of two stages. In the first stage, the PLA/CS polymer is blended with BF to form a hybrid composite as granules. And in the second stage hybrid composite specimens are prepared using injection moulding.

2.3.1 Extrusion of hybrid composites:

Dry PLA, chopped basalt fiber and Chitosan powder were mixed in three different combinations named as PBC1, PBC2, and PBC3 and the details of composition is shown in table 1. This mixture is fed in to high speed co-rotating twin screw extruder for blending and homogeneous mixing. The twin screw extruder has a Screw diameter of 28 mm, L/D ratio of 40, contains 5 different heat zones from feed point to exit point at various heat temperatures 125^0 C, 130^0 C, 140^0 C, 150^0 C, and 165^0 C, respectively. The screw speed is maintained at 150 rpm. Homogeneous mixing of PLA/CS matrix and Basalt fiber was carried out by twin screw extruder for 15 min and then extruded at the ratio f 10 mm/ sec through a 1 mm gauge strands die. Strands were cooled in a water bath and then fed in to pelletizer to make compound pellets. Compounded pellets were dried at 60^0 C in a vacuum for 12 hrs and stored in an air tight container.

2.3.2 Preparation of hybrid composite specimens:

The PLA/BF/CS compounded pellets were processed by injection moulding at a melt temperature of 170 ^{0}C, back pressure of 7 bar, screw speed of 60 mm/ sec and mould temperature of 30^0C. Screw diameter 30 mm with L/D ratio of 20 is used to obtain hybrid composite specimen in the Injection moulding machine. Test specimens for wear test as per ASTM G 99 standard. The test specimens were subjected to annealing at a temperature of 80^0C

ISSN 2394-3777 (Print)
ISSN 2394-3785 (Online)
Available online at www.ijartet.com
International Journal of Advanced Research Trends in Engineering and Technology (IJARTET)
Vol. 3, Special Issue 22, April 2016

in an oven for 24 hours.

2.4. Wear Tests

A pin-on-disc type apparatus was used to investigate the dry sliding frictional and wear behavior of the composite material according to ASTM G 99 test standard. The specimen attached pin is mounted on to the arm of tribometer. During the wear tests, the end surface of the specimen pins were pressed against a horizontal rotating cast iron. The sample is made to rotate on the wear disc made of cast iron with 55mm diameter and 10mm thick. Different loads in the range of 10 N to 40 N were applied directly on the top of the pin and the sliding velocities were varied from 0.104 to 0.523 m/s for a period of 15min. The friction coefficient was calculated from the friction force measured during the wear test, and the wear rates are calculated in microns as displayed by the tester. Also the temperature at the contact surface is recorded. The worn surfaces of the composite specimen were analyzed in order to investigate the operating wear mechanisms by JEOL Scanning Electron Microscope [SEM].

3. Results and Discussions

3.1. Development of Wear Mechanism Map by Fuzzy Clustering Method

Wear rate of the hybrid composites with respect to sliding velocity and normal force were studied using wear rate map represented by contours. The change of contour lines indicates the change of wear mode (mild wear to severe wear. MATLAB software is used to navigate the wear rate map, taking sliding velocity on X-axis and normal force on Y – axis and average wear rate on Z – axis.

Wear transmission map or wear mechanism map is developed from the wear rate map. The boundaries of maximum wear and their transitions are the important data in drafting the wear map, doing this may change the wear rate [17]. The boundaries in wear mechanism map separate the nature of wear as mild wear, severe wear and ultra severe wear.

The mild wear regime of any composite is considered to be acceptable for application purpose, whereas severe and ultra severe are unacceptable values. Fuzzy C means algorithm is uses to identify the boundaries in wear mechanism [18]. The Fuzzy C-means clustering algorithm uses the minimization of the fuzzy C-means functional. The three input parameters used are: param: c, as the number of clusters or initializing partition matrix; param:s, as the fuzziness weighting exponent; and param:e, as the maximum termination tolerance. The two parameters s and e have their default value, if the user does not give them. The standard Euclidean distance norm was calculated by function where the norm inducing matrix is a nE`n identity matrix. The result of the partition is collected in structure arrays. At each iteration step the partition matrix cluster centers, the

ISSN 2394-3777 (Print)
ISSN 2394-3785 (Online)
Available online at www.ijartet.com
International Journal of Advanced Research Trends in Engineering and Technology (IJARTET)
Vol. 3, Special Issue 22, April 2016

square distances, the number of iterations, and the values of the C-means functional can be obtained.

The boundaries of each wear regime were found out by fuzzy clustering technique. Hence the boundaries between the wear regimes were drawn by removing the intermediate contours of the wear rate map [19].

3.2. Friction and Wear characteristics of PBC1

Fig. 1a shows the wear behavior of PBC1 with respect to normal force and sliding velocity. At all sliding velocities the wear rates are found to increase with increasing normal force. Similarly in Fig. 1 b, the coefficient of friction increases with increase in normal force and sliding velocity. From Fig. 2, it can be seen that transition of wear mechanism changes with increasing normal force. The mild wear regime of PBC1 has a maximum wear rate of 140 microns and a maximum coefficient of friction of 0.47, which is well supported by the micrographs of worn out specimens shown in Fig. 2a. The dominant wear mechanism in the regime is ironing mechanism that contributed to higher wear resistance due to strong bond between the fiber and the matrix made the material separation from the pin more difficult [20].

When the load was increased beyond 20N, the speed was maintained at 2.62 m/s, the wear regime shifted from mild wear to severe wear which has a maximum wear rate of 280 microns and a maximum coefficient of friction of 0.490. In this regime, there was a considerable increase in coefficient of friction and wear rate which may be due to elastic deformation of surface asperities due to increasing contact temperature. The SEM photography of worn out specimens shown in Fig. 2b reveals the presence of matrix fracture and ploughing mechanisms. The above statement is well correlated with the studies of Ming Qui Zhang et.al [291. This mechanism was predominant in the severe wear regime with higher loads and a low sliding velocity. Repeated ploughing and matrix fracture causes surface fatigue occurred in a small proportion of the displaced material that was detached from the surface [22].

When the loading conditions were increased beyond 40N, transition of wear regime from severe wear to ultra-severe wear took place. The wear rates in the ultra severe wear regime exceeded 424.54 microns and the corresponding coefficient of friction is more than 0.53. SEM micrographs of worn out specimens in the ultra severe regime shown in Fig. 2c confirms the presence of matrix damage and deep ploughing mechanisms.

3.3. Friction and Wear Characteristics of PBC2

ISSN 2394-3777 (Print)
ISSN 2394-3785 (Online)
Available online at www.ijartet.com
International Journal of Advanced Research Trends in Engineering and Technology (IJARTET)
Vol. 3, Special Issue 22, April 2016

Fig. 3a and 3b represents the effect of sliding velocity and normal force on the wear rate of PBC2. The wear rate of the specimen increases with increase in normal force and follows the increasing trend until the normal force reaches the value of 20 N. The wear rate started to increase gradually with normal force as shown in Fig.3a, whereas the coefficient of friction increases with increase in normal force which is shown in Fig.3b. From the wear mechanism map shown in Fig. 4a, it can be observed that the mild wear regime exists at low normal forces for all sliding velocities [23-24]. In this regime a maximum wear rate of 200 microns and a maximum coefficient of friction of 0.52 were obtained respectively. From the micrographs of worn out specimen taken at mild wear regime, it is clearly seen the dominance of ploughing mechanism and matrix fracture where the bulk of materials recovers elastically which may be due to localized decrease in roughness [25]. The severe wear regime was dominated by deep ploughing and matrix damage mechanism shown in Fig. 4b. For severe wear regime the wear rate values ranges from 200 microns to 400 microns whereas the coefficient of friction values ranges from 0.52 to 0.68.

The ultra severe wear regime shown in Fig. 4c, displays the dominance of fiber-matrix debonding and fiber fracture mechanism is greatly observed. The corresponding values of wear rate and coefficient of friction have exceeded 538.54 microns and 0.72 respectively. In comparison with PBC1, the wear rate of PBC2 has greatly increased, that is the maximum wear rate of PBC1 in mild wear is 140 microns whereas the maximum wear rate of PBC2 in mild wear regime is 200 microns. As the temperature of contact surfaces are not uniform the thermal gradients developed have generated thermal stresses in the specimen which leads to weakening of fiber matrix damage at interface. Fibers become loose and shear easily due to repeated axial thrust during sliding [26-28].

The results also suggest that the wear rate is highly determined by the type or ingredients of the friction material. On micro scale, the friction and wear characteristics of friction material depend on the formation, growth, disintegration of contact plateaus, shape adaption and thermal induced deformation [29].

3.4. Friction and Wear characteristics of PBC3

Fig. 5a and 5b shows the influence of sliding velocities and normal force on the wear rate and coefficient of friction of PBC3 respectively. The wear rates decreases with normal force up to a normal force of 20 N for all sliding velocities. Beyond this, the wear rates follow the increasing trend with normal force. At lower sliding velocities, the coefficient of friction decreases with increasing normal force, whereas for the sliding velocities of 1.96 m/s

ISSN 2394-3777 (Print)
ISSN 2394-3785 (Online)
Available online at www.ijartet.com
International Journal of Advanced Research Trends in Engineering and Technology (IJARTET)
Vol. 3, Special Issue 22, April 2016

and above the coefficient of friction increases with increase in normal force.

Fig. 6 shows the wear mechanism map of PBC3 with respect to normal forces and sliding velocity. The mild wear regime has a maximum wear rate of 240 microns and maximum coefficient of friction of 0.898. Fig. 6a shows a dominance of matrix damage and deep crack in the mild wear regime [30]. The severe wear regime of PBC3 composites have the wear rates ranging from 240 to 480 microns whereas the coefficient of friction varies from 0.898 to 0.91. SEM images of worn out specimens in the severe wear regime shown in Fig. 6b, shows the dominance of matrix debonding and deep ploughing mechanism. The ultra-severe regime have the wear rates above 12.4 microns and a coefficient of friction of 0.93 which causes the wear through fracture matrix debonding and fiber fracture shown in Fig. 6c.

3.5 Dependence on Contact Temperature on Normal Force and Sliding Velocity

Contact temperatures with respect to normal velocities of PBC1 composite under dry sliding is shown in Fig.7a, 7b and 7c. The graphs show the contact temperature increases with increase in sliding velocities. The increase in load results in rise in frictional heat [31]. When the load increases from 10 N to 40 N a gradual increase in temperature noticed. Maximum contact temperature of 23.95˚C recorded in PBC1, 25.87˚C for PBC2 and 26.90˚C for PBC3, when the speed is 3.27 m/s and load is 40 N.

There is no remarkable difference in temperature gradient when the speed increases from 0.628 to 3.27 m/s. When the force is increased, there is a rise in temperature which is due to frictional heating of contacting surfaces. The mechanical energy converts in to heat is a dissipation process of friction behavior. The transformation of mechanical energy into heat can be attributed to the origination of the breakdown of adhesion bonds, transferring behavior of the materials and plastic deformation.

From the study, it is found that the PBC1 has a maximum wear rate of 140 microns in the mild wear regime while the PBC2 and PBC3 have their maximum wear rates of 200 and 240 microns respectively. The maximum wear rate in the severe wear regimes of PBC1, PBC2 and PBC3 are 280, 400 and 480 microns respectively. Hence, the PBC1 composites showed better wear resistance pattern in comparison with PBC2 and PBC3 composite. As the weight percentage of basalt fiber and chitosan increases in PLA matrix shows better wear rate when compared to PBC2 and PBC3. The contact temperature of PBC1 seems to be low compared to PBC2 and PBC3, shows low friction heat in PBC1. Also good thermal characteristics and bonding nature of basalt fibers and chitosan polymers make PBC1 a material with good wear resistance.

ISSN 2394-3777 (Print)
ISSN 2394-3785 (Online)
Available online at www.ijartet.com
International Journal of Advanced Research Trends in Engineering and Technology (IJARTET)
Vol. 3, Special Issue 22, April 2016

4. Conclusions

From the results and discussion above the following conclusions can be made:

1. The increase in weight percentage of basalt fiber in the polylactic acid/chitosan matrix as a reinforcement increases the wear resistance of the composites.

2. The wear rate increased with increases in applied load from 10 to 40 N and coefficient of friction also increases with normal velocity when it increased from 1.31 to 3.27 m/s.

3. It is observed that fibers are mostly affected at higher magnitudes of force and sliding velocities in the regimes of severe wear and ultra-severe wear.

4. Ironing and ploughing mechanism are noticed maximum in the mild wear regime of wear mechanism map whereas deep ploughing and matrix fracture are mostly seen in severe wear regime. The ultra severe regime was dominated by fiber matrix debonding and fiber fracture.

5. Comparative study of wear rate of three composites, PBC1 is found to be a better choice for the wear resistant composite that can be suitable for engineering and medical application.

6. The wear mechanism map developed using Fuzzy Clustering method proved to be an effective tool in the study of wear behavior of materials.

7. The lowest contact temperature is recorded for PBC1 compared to PBC2 and PBC3, shows that lowered frictional heat and wear rates in PBC1.

REFERENCES

1. Ren X. Biodegradable plastics: A solution of a challenge? : Journal of Cleaner Production; 2003. Vol.11, pp 27-40.
2. Martin O, Averous L. Poly(lactic acid):plasticization and properties of biodegradable multiphase systems: Polymer; 2001. Vol. 42, pp 6209-6219.
3. Yu L, Dean K, Li L. Polymer blends and composites from renewable resources: Progress in Polymer Science; 2006. Vol. 31, pp 576-602.
4. Christo Ananth, S.Esakki Rajavel, S.Allwin Devaraj, M.Suresh Chinnathampy. "RF and Microwave Engineering (Microwave Engineering)." (2014): 300.
5. Chin CW, Yousif BF. Tribological behavior of KFRE Composite. Wear**267**: 1550-1557, 2009.
6. Sangthon GS, Pongprayoon T, Yanume TN. Mechanical property improvement of unsaturated polyster composite reinforced with admicellar treated sisal fibers. Composites part A **40**: 687-694, 2009.
7. Plackett D, Andersen TL, Pedersen WB, Nielsen L. Biodegradable composites based on lpolylactide and jute fibres:

ISSN 2394-3777 (Print)
ISSN 2394-3785 (Online)
Available online at www.ijartet.com
International Journal of Advanced Research Trends in Engineering and Technology (IJARTET)
Vol. 3, Special Issue 22, April 2016

Composites Science and Technology; 2003. Vol. 63, pp 1287-1296.

8. Tabi T, Kovacs G. Examination of starch pre-process drying and water absorption on injection moulded poly(lactic acid)/starch blends: Polymer Engineering and Science; 2011.Vol. 51, pp 843-850.

9. Gurev VV, Neproshin EI, Mostovoi GE. The effect of basalt fiber production technology on mechanical properties of fiber: Glass and Ceramics; 2001.Vol. 58, pp 62-65.

10. Kogan FM, Nikitina OV. Solubility of chrysotile asbestos and basalt fibers in relation to their fibrogenic and carcinogenic action Environ: Health Perspect; 1994.102, 205–6.

11. Swetha, M.; Sahithi, K.; Moorthi, A.; Srinivasan, N.; Ramasamy, K.; Selvamurugan, N.

Biocomposites containing natural polymers and hydroxyapatite for bone tissue engineering. Int. J. Biol. Macromol. 2010, 47, 1-4.

12. Kim, I.Y.; Seo, S.J.; Moon, H.S.; Yoo, M.K.; Park, I.Y.; Kim, B.C.; Cho, C.S. Chitosan and its derivatives for tissue engineering applications. Biotechnol. Adv. 2008, 26, 1-21.

13. Cuero RG. Antimicrobial action of exogenous chitosan. In: Jolles, P., Muzzarelli, R.A.A., (Eds.), Chitin and Chitosan. Birkhauser Verlag, Basel, Siwitzerland; 1999. pp. 315–333.

14. Madugu IA, Abdulwahab M, Aigbodion VS. Effect of iron fillings on the properties and microstructure of cast fiberpolyester/iron fillings particulate composite. J Alloys Comp 2007; 476:807e11.

15. Hornsby PR, Hinrichsen E, Tarverdi K. Preparation and properties of polypropylene composites reinforced with wheat and flax straw fibers. J Mater Sci 1997;32(2):443e9.

16. Sangthon GS, Pongprayoon T, Yanume TN. Mechanical property improvement of unsaturated polyster composite reinforced with admicellar treated sisal fibers. Composites part A **40**: 687-694, 2009

17. Williams JA.Wear Modeling: Analytical, Computational and Mapping: A Continuum Mechanics Approach.Wear**1**: 225-229(1999)

18. BezdekJC.Pattern Recognition with Fuzzy Objective function Algorithms.Plenum Press: (1981)

19. Srinivasan V, Mohamad Rafi N, Karthikeyan R, KalaiSelviV. Characteristics of Al2O3 Nano-filled

ISSN 2394-3777 (Print)
ISSN 2394-3785 (Online)
Available online at www.ijartet.com
International Journal of Advanced Research Trends in Engineering and Technology (IJARTET)
Vol. 3, Special Issue 22, April 2016

GFRP Composites Using Wear Maps. Journal of Reinforced Plastics andComposites**29**: 3006-3015 (2010)

20. Schwartz CJ, BahadurS. The Role of Filler Deform Ability, Filler-Polymer Bonding And Counter Material on The Tribological Behavior of Polyphenylene Sulfide (PPS).Wear**251**:1532-1540(2001)

21. Ming Qui Zhang, Min ZhiRong, ShuLiYu, Bernd Wetzel, Klaus Friedrich. Effect of Particle Surface Treatment on the Tribological Performance of Epoxy Based Nano composites. Wear**253**:126-136(2002)

22. Myshkin N, Kipetrokovets M, and KovalevAV.Tribology of Polymers: Adhesion, Friction, Wear and Mass Transfer.Tribology International**38**: 910-921(2005)

23. Davim JP, RosariaC. Effect of Reinforcement (Carbon or Glass Fiber) on Friction and Wear Behavior of the Peek against Steel Surface at Long Dry Sliding.Wear**266**: 795-799(2009)

24. Chauhan SR, KumarA, Singh I. Sliding Friction and Wear Behavior of Vinyl esterand Its Composites Under Dry and Water Lubricated Sliding Conditions. Materials & Design**31**:2745-2751 (2010)

25. QuintelierJ, De Baets P, Samyn P, Van Hemelrijck D. On the SEM features Glass Polyester Composite system subjected to Dry sliding wear.Wear**261**: 703-714(2006)

26. Pramendra Kumar Bajpai, Inderdeep Singh, JitendraMadaan. Tribological Behavior of Natural Fiber Reinforced PLA Composites.Wear**297**:829-840(2012)

27. SumerM, UnalH, MimarogluA. Evaluation of Tribological Behavior of Peek and Glass Fiber Reinforced Peek Composite under Dry Sliding and Water Lubricated Conditions.Wear**265**: 1061-1065 (2008)

28. YousifBF, EI-TayebNSM.Wear and Friction Characteristics of CGRP Composite under Wet Condition Using Two Different Test Techniques.Wear**265**: 856-864 (2008)

29. El-TayebNSM.Abrasive Wear Performance of Untreated SiCp Reinforced Polymer Composite.Journal of Materials Processing Technology**206**: 305-314(2008)

30. Mohamed RaffiN, SrinivasanV.A Study on Wear Behavior of Γ-Uhmwpe Sliding Against 316l Stainless Steel Counter Surface.Wear**306**: 22-26(2013)

ISSN 2394-3777 (Print)
ISSN 2394-3785 (Online)
Available online at www.ijartet.com
International Journal of Advanced Research Trends in Engineering and Technology (IJARTET)
Vol. 3, Special Issue 22, April 2016

31. Mohan, S., Prakash, V., and Pathak, J. P. (2002). Wear Characterisitics of HSLA Steel, Journal of Wear, 252: 16–25.

TABLES

Table.1 Weight percentage of Hybrid composites

SAMPLES	WEIGHT PERCENTAGE PLA : BS : CS
PBC1	65 : 25 : 10
PBC2	75 : 15 : 10
PBC3	85 : 10 : 5

ISSN 2394-3777 (Print)
ISSN 2394-3785 (Online)
Available online at www.ijartet.com
International Journal of Advanced Research Trends in Engineering and Technology (IJARTET)
Vol. 3, Special Issue 22, April 2016

FIGURE CAPTIONS

Figure 1 a Effect of normal force and sliding velocity on wear rate of PBC1

Figure 1 b Effect of normal force and sliding velocity on COF of PBC1

Figure 2 Wear mechanism map for PBC1 composites

Figure 3 a Effect of normal force and sliding velocity on wear rate of PBC2

Figure 3 b Effect of normal force and sliding velocity on COF of PBC2

Figure 4 Wear mechanism map for PBC2 composites

Figure 5 a Effect of normal force and sliding velocity on wear rate of PBC3

Figure 5 b Effect of normal force and sliding velocity on COF of PBC3

Figure 6 Wear mechanism map for PBC3 composites

Figure 7 a Effect of normal force and sliding velocity on contact temperature of PBC1

Figure 7 b Effect of normal force and sliding velocity on contact temperature of PBC2

Figure 7 c Effect of normal force and sliding velocity on contact temperature of PBC3

ISSN 2394-3777 (Print)
ISSN 2394-3785 (Online)
Available online at www.ijartet.com
International Journal of Advanced Research Trends in Engineering and Technology (IJARTET)
Vol. 3, Special Issue 22, April 2016

FIGURES

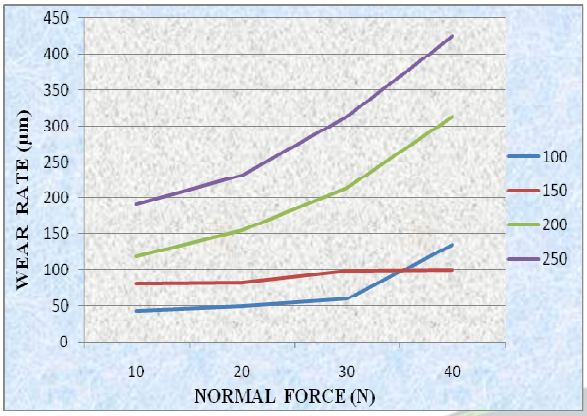

Figure 1 a Effect of normal force and sliding velocity on wear rate of PBC1

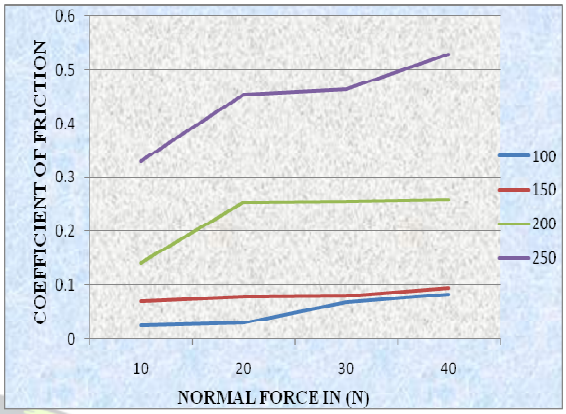

Figure 1 b Effect of normal force and sliding velocity on COF of PBC1

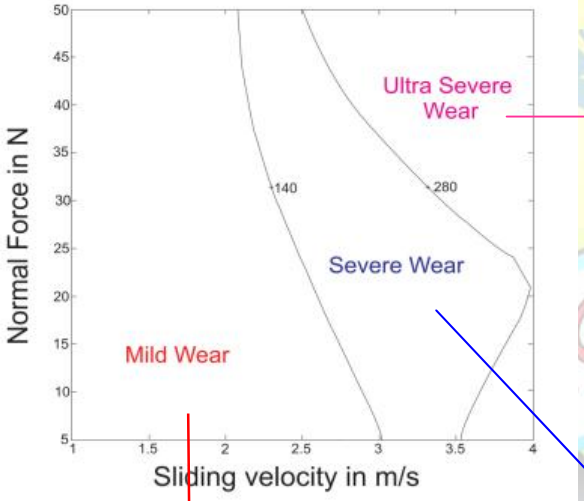

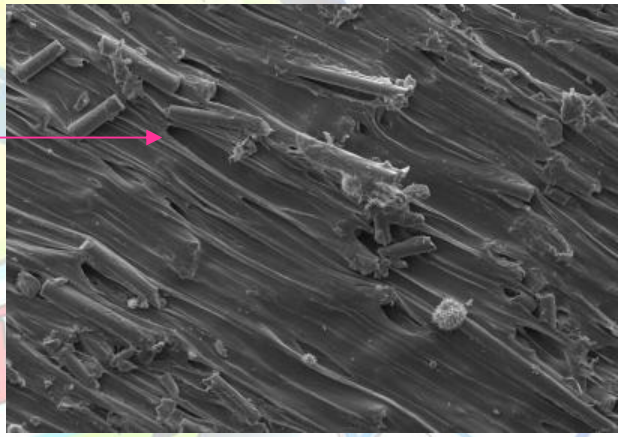

(c)Matrix damage and deep ploughing.

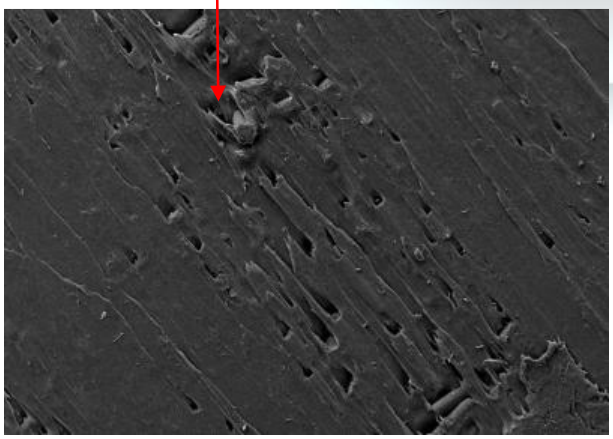

(a)Ironing

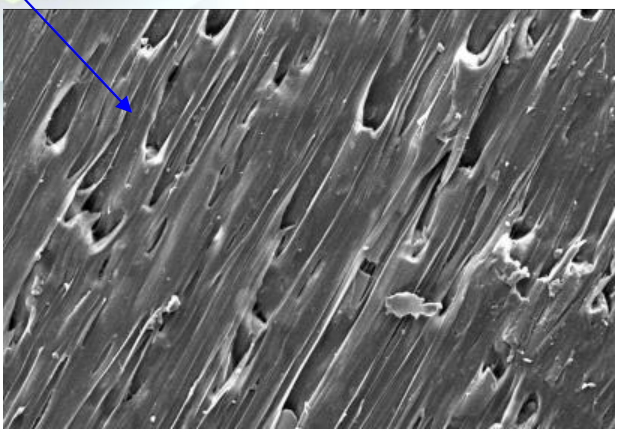

(b)ploughing and matrix fracture

ISSN 2394-3777 (Print)
ISSN 2394-3785 (Online)
Available online at www.ijartet.com
International Journal of Advanced Research Trends in Engineering and Technology (IJARTET)
Vol. 3, Special Issue 22, April 2016

Figure 2 Wear mechanism map for PBC1 composites

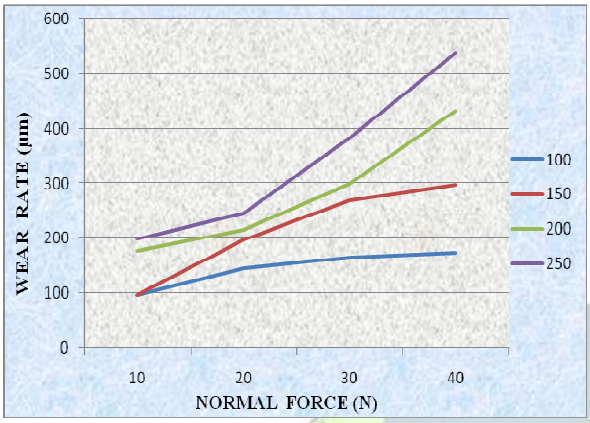

Figure 3a Effect of normal force and sliding velocity on wear rate of PBC2

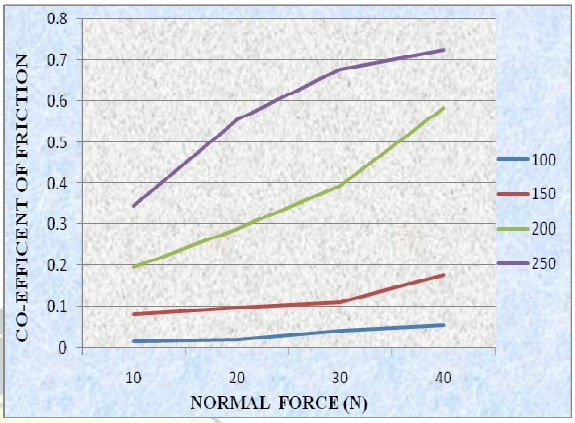

Figure 3b Effect of normal force and sliding velocity on COF of PBC2

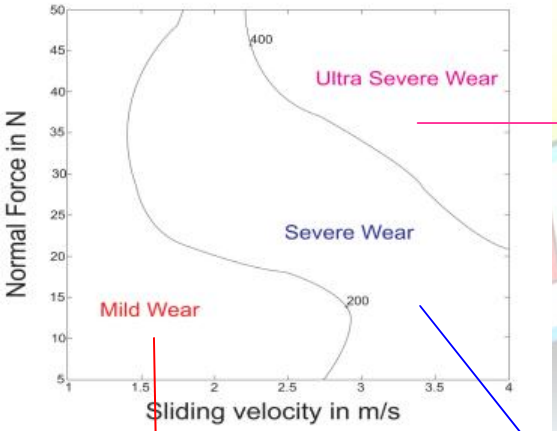

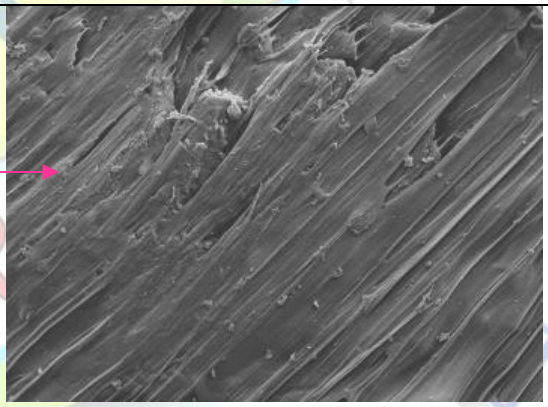

(c) Fiber Fracture mechanism and Matrix debonding

ISSN 2394-3777 (Print)
ISSN 2394-3785 (Online)
Available online at www.ijartet.com
International Journal of Advanced Research Trends in Engineering and Technology (IJARTET)
Vol. 3, Special Issue 22, April 2016

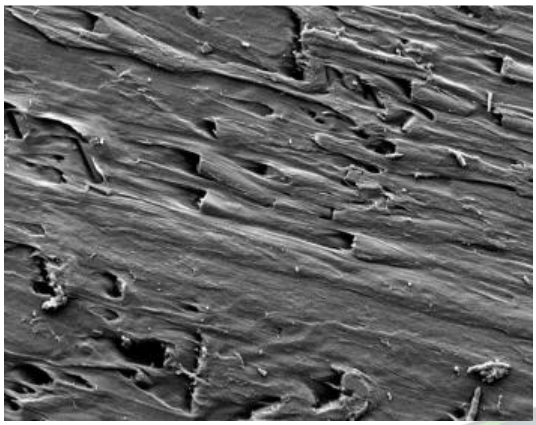

(a) Ploughing and Matrix Fracture Mechanism

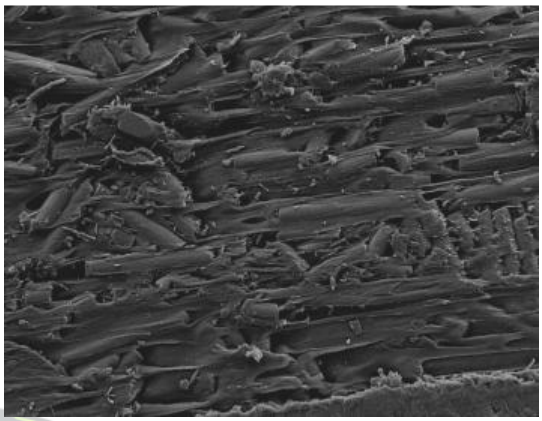

(b) Deep Ploughing and Matrix damage

Figure 4 Wear mechanism map for PBC2 composites

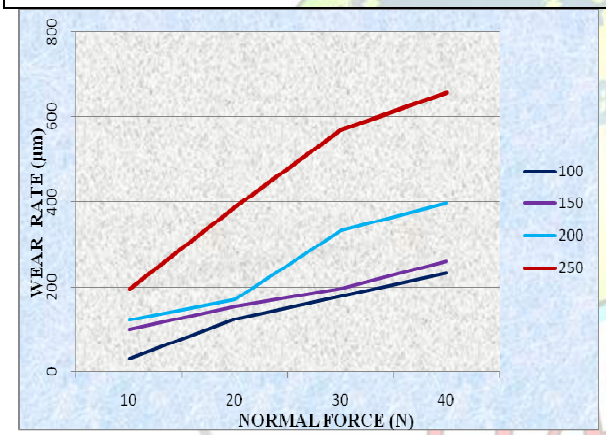

Figure 5 a Effect of normal force and sliding velocity on wear rate of PBC3

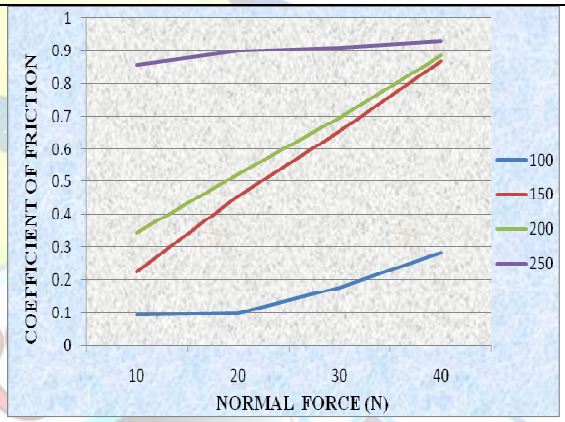

Figure 5 b Effect of normal force and sliding velocity on COF of PBC3

ISSN 2394-3777 (Print)
ISSN 2394-3785 (Online)
Available online at www.ijartet.com
International Journal of Advanced Research Trends in Engineering and Technology (IJARTET)
Vol. 3, Special Issue 22, April 2016

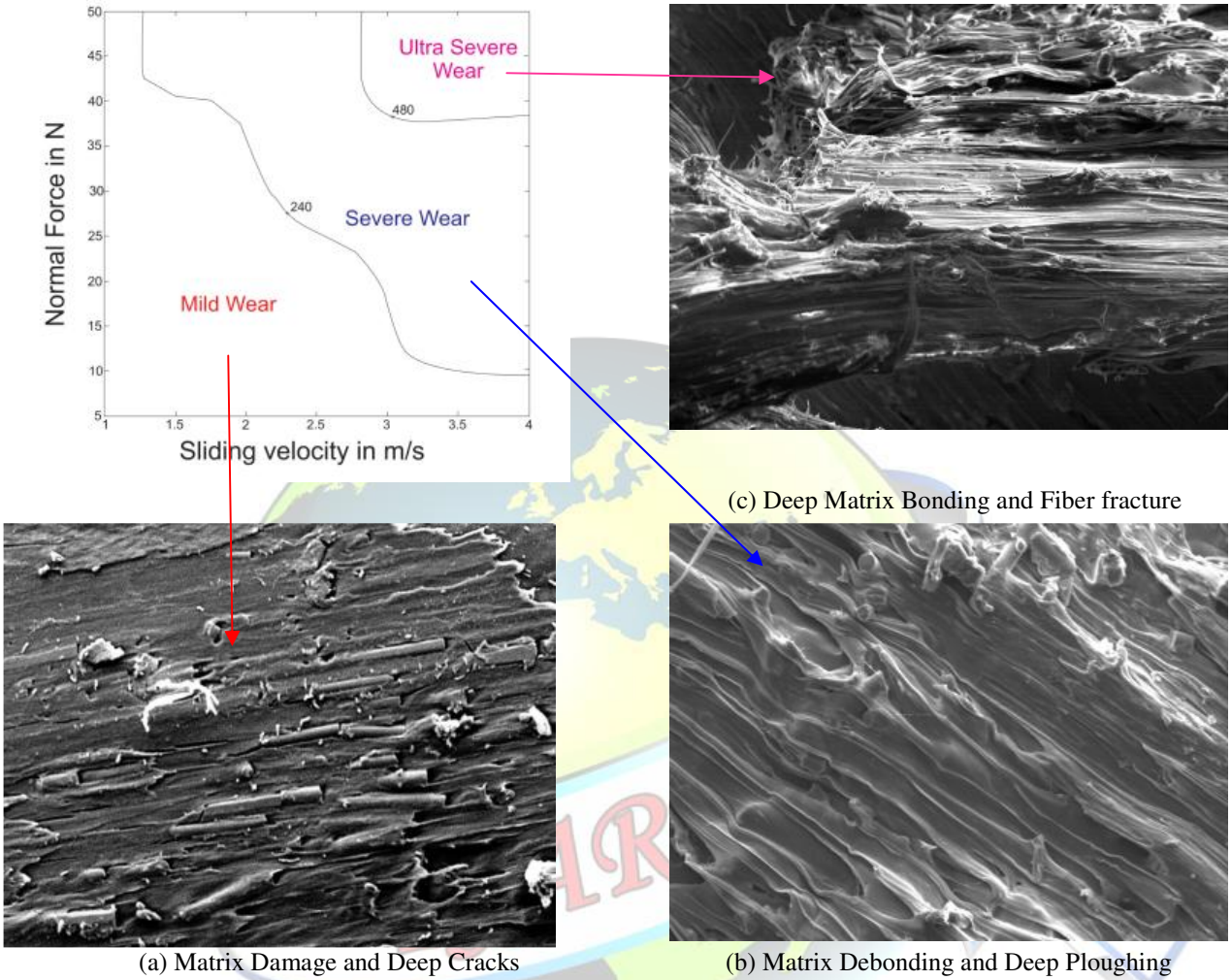

(c) Deep Matrix Bonding and Fiber fracture

(a) Matrix Damage and Deep Cracks

(b) Matrix Debonding and Deep Ploughing

Figure 6 Wear mechanism map for PBC3 composites

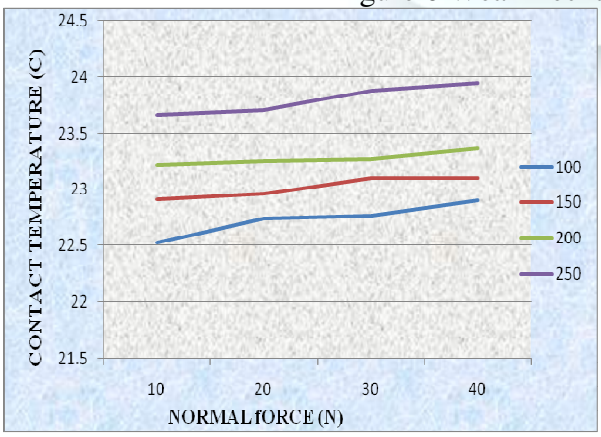

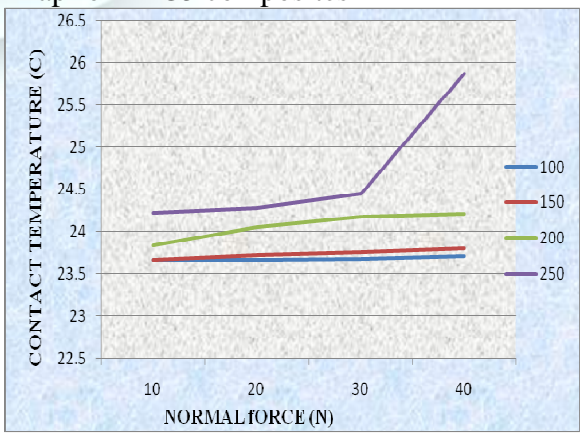

ISSN 2394-3777 (Print)
ISSN 2394-3785 (Online)
Available online at www.ijartet.com
International Journal of Advanced Research Trends in Engineering and Technology (IJARTET)
Vol. 3, Special Issue 22, April 2016

Figure 7a Effect of normal force and sliding velocity on contact temperature of PBC1

Figure 7b Effect of normal force and sliding velocity on contact temperature of PBC2

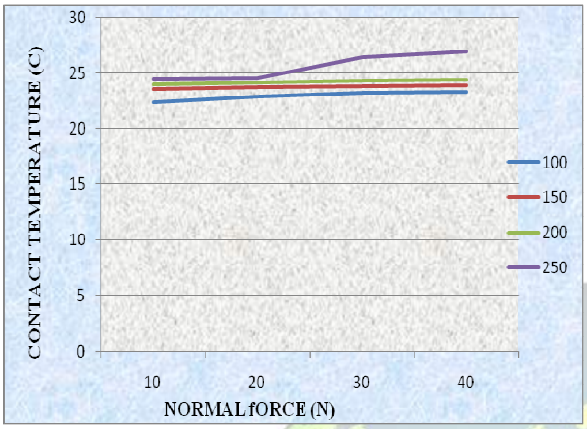

Figure 7c Effect of normal force and sliding velocity on contact temperature of PBC3